

Figure 1 Knot conformations. **a**, Packed Hopf tori. **b**, 'Linear' conformations. Left, a product of trefoils; right, a thick chain with a linear relationship between crossing number and rope length. The chain also seems to be a continuous family of minima for rope length, in which case minima are not isolated in the link class. **c**, 'Linear' conformation of a twist knot – apparent minimum. **d**, An N -crossing knot fits in a square of side order N . **e, f**, Minima for figure-eight and square knot respectively. No particular accuracy is claimed – these knots were tied before the calculation of the computer data⁷, and both the conformation and the values for rope length match almost exactly, as did several other knots. **g**, Minimum for the 'granny' knot, differing in shape from the minimum found by computer⁸, and having a different symmetry. **h**, Another view. We estimate this to be the true global minimum. **i**, Some support for the accuracy of the rope calculations is given by this conformation of the five-crossing torus knot, which by rope seemed to be a lower minimum than the conformation reported in ref. 7. Further computation confirmed this.



shape, scaled so that $R(K)=1$, with total length L . The inverse-square 'energy' ($S(K)$, A , writhe, and so on) can be estimated by assuming the 'mass' of the knot is concentrated at points p on the integer lattice. Concentric shells of unit thickness about each p each contribute the same amount, so the contribution for p is that constant multiplied by the number of shells, which is of the order of $L^{1/3}$. Multiplying by the number of points, L , gives $L^{4/3}$. The proof that $S(K)$ linearly bounds A is simple vector geometry.

The $4/3$ exponent is sharp. Consider the Hopf link of two tori in its natural geometrical position. Fill each torus with N loops parallel to the centre curve, each loop a strand of radius 1 (Fig. 1a). Then with any tight packing of the loops, the minor radii of the tori is of the order of \sqrt{N} . The conformation fits inside a sphere of radius $4\sqrt{N}$, so the total rope length is about $N^{3/2}$. Each loop is linked with N loops in the perpendicular torus, so the crossing number is about N^2 . Therefore the rope length is of the order of $C(K)^{3/4}$. Because $11L(K)^{4/3} \geq 4\pi A(K) \geq C(K)$, this example has A in the order of $L(K)^{4/3}$.

The minimum rope length for a knot is bounded by $3C(K)^2$. This can be seen by arranging the knot so that the crossings are evenly spaced along a line (Fig. 1d). For the simpler knot types, $L(K)$, $S(K)$ and A in minimized conformations all 'appear' to be

linearly related⁷. An explanation is that the simpler conformations are 'planar': from most perspectives a unit arc of the knot crosses only a few other unit arcs.

As complexity increases, there are many families of knots and links with three-dimensional growth, exhibiting the $4/3$ power law. Families with single-dimensional growth (Fig. 1b,c) have a linear relationship among the measures. With planar growth, we expect A to be linear with $C(K)$ and $S(K)$ to be of the order of $L(K)\log L(K)$.

We propose that the rope length required (Fig. 1e–i) to tie an N -crossing knot or link varies only between $k_1 N^{3/4}$ and $k_2 N$. Other investigators have also recently observed the $4/3$ law in knots on the cubic lattice⁹ and in vector fields¹⁰.

A good knot energy has only a finite number of knot types realized below any given energy level. Our theorem gives us this property for $L(K)$ and $S(K)$, proving that there is a finite number of knots that can be tied with a finite length of mathematical rope.

Gregory Buck

Department of Mathematics, Saint Anselm College, Manchester New Hampshire 03102, USA
email: gbuck@anselm.edu

1. Simon, J. in *Mathematical Approach to Biomolecular Structure and Dynamics* (Proc. of 1994 IMA Summer Program on Molecular Biology; eds Mesirov, J. P., Schulten, K. & Sumners,

D.W.) 39–58 (IMA 82, Springer, New York, 1996).

2. Stasiak, A., Katritch, V., Bednar, J., Michoud, D. & Dubochet, J. *Nature* **384**, 122 (1996).
3. Buck, G. & Simon, J. *Topol. Appl.* (in the press).
4. O'Hara, J. *Topology* **30**, 241–247 (1991).
5. Moffatt, H. K. *Nature* **347**, 367–369 (1990).
6. Buck, G. & Orloff, J. *Topol. Appl.* **61**, 205–214 (1995).
7. Katritch et al. *Nature* **384**, 142–145 (1996).
8. Buck, G. (Preprint no. 2, Math. Dept, St Anselm College, 1993).
9. Diao, Y. & Ernst, K. *Topol. Appl.* (in the press).
10. Cantarella, J., DeTurck, D. & Gluck, H. (Preprint, Math. Dept., Univ. Pennsylvania, 1997).
11. Katritch, V., Olson, W. K., Pieranski, P., Dubochet, J. & Stasiak, A. *Nature* **388**, 148–151 (1997).

Heartbeat synchronized with ventilation

It is widely accepted that cardiac and respiratory rhythms in humans are unsynchronized¹. However, a newly developed data analysis technique allows any interaction that does occur in even weakly coupled complex systems to be observed. Using this technique, we found long periods of hidden cardiorespiratory synchronization, lasting up to 20 minutes, during spontaneous breathing at rest.

Synchronization is a universal phenomenon that occurs when two or more nonlinear oscillators are coupled. It is observed in many fields of science and is widely applied in engineering. The case of synchronization in periodic, or even noisy, oscillators is well understood^{2–4}. The notion of synchronization has often been used to analyse the interaction between physiological (sub)systems¹, but these studies have been restricted to almost periodic rhythms. No approach has been suggested to probe the weak interactions between such irregular and non-stationary oscillators as the human heart and respiratory system.

These two physiological systems are known to be coupled by several mechanisms, but apart from respiratory modulation of heart rate, first observed in 1847 and known as 'respiratory sinus arrhythmia' (RSA)^{5–7}, no other effects have been reported. Moreover, in spite of some early communications⁸, it has been concluded that "there is comparatively weak coupling between respiration and the cardiac rhythm, and the resulting rhythms are generally not phase locked"¹.

We used the concept of phase synchronization of chaotic oscillators^{9,10} to develop a technique to analyse irregular non-stationary bivariate data. We analysed data obtained in non-invasive examinations of eight healthy volunteers (14–17-year-old, high-performance swimmers; four of them male and four female). While subjects lay at rest, electrocardiograms (ECGs) were recorded while respiratory

Table 1 Subjects, ordered by the amplitude of respiratory sinus arrhythmia (RSA) determined as the averaged difference between the longest and shortest R–R interval within every respiratory cycle*

Code	Sex	Age	R–R (ms)		Resp. cycle (ms)		RSA (ms)		Synchronization
			Median	Δ Quart.	Median	Δ Quart.	Median	Δ Quart.	
A	m	16.1	1,104	28	3,110	390	15	40	3:1 (1,000 s), 5:2 (300 s), 8:3 (20 s)
B	m	14.6	1,018	95	3,210	610	31	38	3:1 (several spells of 40 s)
C	m	13.9	975	110	3,230	850	46	57	3:1 (20 s), 7:2 (20 s), 4:1 (20 s)
D	f	15.2	1,157	157	2,930	780	56	57	5:2 and 3:1 (several spells of 30 s)
E	m	16.9	1,026	89	3,650	620	67	47	7:2 (60 s), 3:1 and 4:1 (20s)
F	f	15.0	1,024	143	2,960	700	74	75	11:4 (20 s)
G	f	15.9	733	70	5,615	1,550	83	70	No synchronization detectable
H	f	16.3	1,256	197	4,260	2,100	264	296	No synchronization detectable

*If an R–R interval spans two adjacent cycles, it is considered to belong to that one which contains more than 50% of the interval. For R–R intervals, respiratory cycles and the RSA, the medians of respective distributions and differences between the first and third quartile (Δ Quart.) are given. We observe that cardiorespiratory synchronization tends to become weak with increasing RSA.

flow was simultaneously measured with a thermistor at the nose. Both signals were digitized with a 1,000-hertz sampling rate and 12-bit resolution. Each record lasted 30 minutes.

The resulting time series were irregular, strongly non-stationary and noisy. These characteristics made it inappropriate, in analysing the mutual dependencies involved, to use even sliding versions of traditional spectral and correlations techniques, or direct computation of instantaneous phase differences^{9,10}. So instead of these techniques, we used a new kind of data presentation which we call a cardiorespiratory synchrogram (CRS), to detect different synchronous states and transitions between them.

We first used the Hilbert transform⁹ to calculate the instantaneous phase $\phi_i(t)$ of the respiratory signal. $\phi_i(t)$ is defined on the real line (not restricted to the $[0, 2\pi]$ interval). Next, we regarded the respiratory

phase stroboscopically at times t_k , where the R-peak in the k th heartbeat occurs and hence the phase of the heart rhythm increases by 2π . In the simplest case of $n:1$ synchronization, there are n heartbeats in each respiratory cycle; these beats appear at n certain values of respiratory phases, which are constant over all cycles.

Plotting these relative phases ψ as a function of time shows n horizontal stripes. In the general case of $n:m$ synchronization, such a structure appears if we relate the phases of the heart beats to the beginning of m adjacent respiratory cycles, $\psi(t_k) = (\phi_i(t_k) \bmod 2\pi m) / 2\pi$; we have n horizontal stripes within m respiratory cycles.

This technique allows us to distinguish between different periods of synchronization, even for noisy and non-stationary data. For example, we observe 5:2 locking between the respiratory frequency ω_r and the heart rate ω_h ($5\omega_r \approx 2\omega_h$) during a

period of about 300 seconds, then after a transition period, a regime of 3:1 phase locking is found for about 20 minutes (Fig. 1). These two kinds of locking can be recognized using histograms (Fig. 1c) and the autocorrelation function of phases (Fig. 1d).

Our analysis showed cardiorespiratory synchronization of several locking ratios occurring in six out of eight subjects (Table 1). Subjects with the strongest synchronization had no remarkable RSA, whereas both subjects with the highest RSA exhibited no synchronization.

We conclude that phase locking of respiratory and the cardiac rhythms, and respiratory modulation of heart rate, are two competing aspects of cardiorespiratory interaction. From a physical viewpoint, synchronization and modulation are different phenomena and are related to different coupling. RSA generation is associated mainly with the baroreflex feedback loop and its respiratory phase-dependent information processing⁷.

Perhaps cardiorespiratory synchronization is an expression of another kind of cardiorespiratory interaction, such as a central coupling between cardiovascular and respiratory neuronal activities.

Carsten Schäfer, Michael G. Rosenblum, Jürgen Kurths

Department of Physics, University of Potsdam, Am Neuen Palais 10, PF 601553, 14415 Potsdam, Germany

e-mail: carsten@agnld.uni-potsdam.de

Hans-Henning Abel

Department of Cardioanaesthesiology, Städt Klinikum Braunschweig, Salzdahlumer Strasse 90, 38126 Braunschweig, Germany

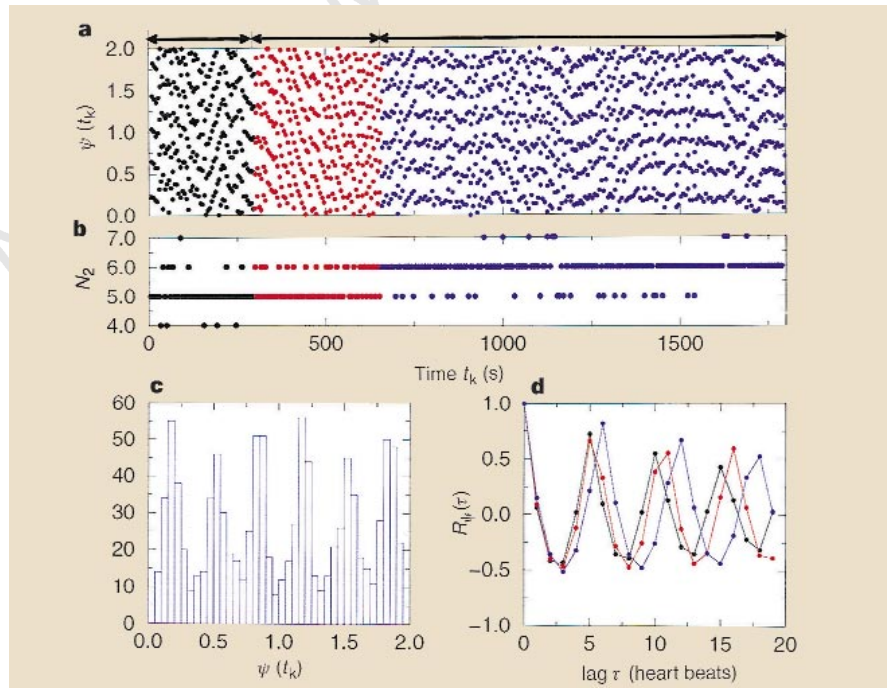


Figure 1 Analysis of cardiorespiratory cycles. **a**, Cardiorespiratory synchrogram, showing the transition (red) from 5:2 frequency locking (black) to 3:1 phase locking (blue). Each point shows the normalized relative phase of a heartbeat within two adjacent respiratory cycles $\psi(t_k) = (\phi_i(t_k) \bmod 4\pi) / 2\pi$. **b**, Number of heartbeats within two adjacent respiratory cycles. **c**, Histogram of phases. The six horizontal stripes in the blue region of the CRS result in six well-pronounced peaks in the distribution of phases. **d**, Autocorrelation function of phases $R_\psi(\tau) = \sum_i (\psi(t_k) - \langle \psi \rangle) (\psi(t_{k+\tau}) - \langle \psi \rangle) / \sum_i (\psi(t_k) - \langle \psi \rangle)^2$. The coloured curves correspond to respective regions.

- Mackey, M. C. & Glass, L. *From Clocks to Chaos: The Rhythms of Life* Ch. 7 (Univ. Press, Princeton, 1988).
- Stratonovich, R. L. *Topics in the Theory of Random Noise* (Gordon and Breach, New York, 1963).
- Blekhman, I. I. *Synchronization in Science and Technology* (ASME, New York, 1988).
- Strogatz, S. H. & Steward, I. *Sci. Am.* **269**, 102–109 (1993).
- Ludwig, C. *Arch. Anat. Physiol.* **13**, 242–302 (1847).
- Anrep, G. V., Pascual, W., Rössler, R. *Proc. R. Soc. Lond. B* **119**, 191–230 (1936).
- Eckberg, D. L., Kifle, Y. T., Roberts, V. L. *J. Physiol., Lond.* **304**, 489–502 (1980).
- Pessenhofer, H. & Kenner, T. *Pflügers Arch.* **355**, 77–83 (1975).
- Rosenblum, M. G., Pikovsky, A. S., Kurths, J. *Phys. Rev. Lett.* **76**, 1804–1807 (1996).
- Pikovsky, A. S., Rosenblum, M. G., Osipov, G. V., Kurths, J. *Physica D* **104**, 219–238 (1997).